MAX PLANCK INSTITUTE
FOR HUMAN DEVELOPMENT

Terms of use:

Provided by:

Behavioral/Cognitive

Out of Rhythm: Compromised Precision of Theta-Gamma Coupling Impairs Associative Memory in Old Age

Anna E. Karlsson,[1,2] **Ulman Lindenberger,**[1,3] **and Myriam C. Sander**[1]

[1]Center for Lifespan Psychology, Max Planck Institute for Human Development, 14195 Berlin, Germany , [2]Department of Psychology, Humboldt-Universität zu Berlin, 12489 Berlin, Germany, and [3]Max Planck UCL Centre for Computational Psychiatry and Ageing Research, 14195 Berlin, Germany, and London WC1B 5EH, England

Episodic memory declines with advancing adult age. This decline is particularly pronounced when associations between items and their contexts need to be formed. According to theories of neural communication, the precise coupling of gamma power to the phase of the theta rhythm supports associative memory formation. To investigate whether age differences in associative memory are related to compromised theta-gamma coupling, we took EEG recordings during the encoding phase of an item-context association task. Fifty-eight younger (33 females) and 55 older (24 females) adults studied pictures of objects superimposed on background scenes. In a recognition test, objects were presented on old or new backgrounds, and participants responded if they had seen (1) the object and (2) the object/scene pair. Theta-gamma coupling supported pair memory formation in both age groups. Whereas pair memory was associated with coupling closer to the peak of the theta rhythm, item-only memory was associated with a deviation in phase angle relative to pair memory. Furthermore, a stable relation between coupling phase and pair memory performance demonstrated that coupling closer to the peak is beneficial for associative memory. Critically, older adults' lower pair memory was accompanied by a shift in coupling phase relative to that of younger adults. In concert, the present results are consistent with the hypothesis that decrements in the temporal precision with which gamma power is coupled to a specific theta phase underlie the decline of associative memory in normal cognitive aging.

Key words: aging; associative memory; cross-frequency coupling; EEG; oscillations

---

Significance Statement

According to prominent theories of neural communication, the precise coordination of oscillatory activity enables the formation of associative memories. We propose that normal cognitive aging impairs associative memory formation by compromising the temporal precision of neural communication. We show that the coupling of high-frequency gamma power to low-frequency theta phase supports associative memory formation in both younger and older adults, with coupling closer to the theta peak benefitting memory performance. However, compared with younger adults, the coupling phase angle is shifted in time and is more variable in the older adults. We conclude that alterations in the precise timing of theta-gamma coupling contribute to adult age differences in associative memory.

Introduction

The principle of Hebbian learning (Hebb, 1949) states that memories are formed via synaptic connectivity, which is modulated by the precise timing of activity between groups of neurons (Markram et al., 1997; Jutras and Buffalo, 2010). Neural oscillations reflect such rhythmic fluctuations in synchronized neural excitability, orchestrating neural communication across different temporal and spatial scales (Fries, 2005; Battaglia et al., 2011; Canolty and Knight, 2010; Buzsáki et al., 2013). High-frequency activity in the gamma band (~40–150 Hz) serves local processing in relatively small cortical neural assemblies over short time windows and has been associated with the representation of item-specific information in the service of memory (Buzsáki and Wang, 2012; Friese et al., 2013; Lisman and Jensen, 2013). In
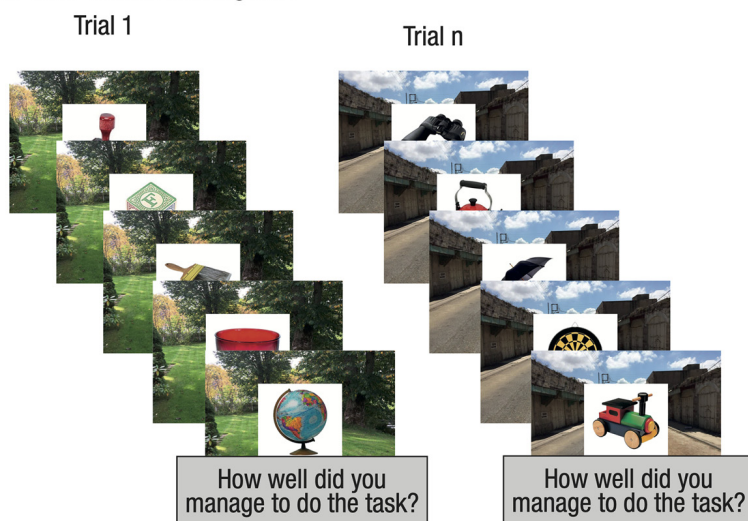
Figure 1. Experimental paradigm. *a*, During learning, participants were presented with objects superimposed on pictures of outdoor scenes and instructed to imagine using the object in the place depicted. *b*, Subsequently, in a surprise recognition memory test, old and new objects were presented on old (matching/mismatching) or new scenes. Participants judged first whether they had seen the object before and then whether they had seen the specific object/scene pair before. Matching scenes corresponded to the scene on which the object was presented during encoding. Mismatching scenes corresponded to old scenes from encoding that were previously paired with another object. The mismatch condition emphasized the need to base the pair memory judgment on the association between the item and the context and not simply on a feeling of familiarity for the constituent elements of the pair.

contrast, low-frequency oscillations in the theta band (~3–8 Hz) integrate information over larger temporal and spatial scales (Sirota et al., 2008; Fell and Axmacher, 2011) by coordinating time windows of synaptic plasticity (Pavlides et al., 1988; Hyman et al., 2003; Hasselmo, 2005) and have been associated with the successful formation (Clouter et al., 2017; Miller et al., 2018; Kota et al., 2020) and retrieval (Guderian and Düzel, 2005; Yaffe et al., 2014; Herweg et al., 2020) of associative memories. Importantly, the coordination of these brain rhythms, namely the coupling of gamma power along the phase of the theta oscillation [i.e., theta-gamma cross-frequency coupling (CFC)] has been demonstrated to underlie the successful formation of memories contingent on contextual information (Tort et al., 2009; Staudigl and Hanslmayr, 2013; Heusser et al., 2016; Köster et al., 2018). Thus, theta phase coding presumably provides a key mechanism for the formation of item-context associations during memory encoding (Hanslmayr et al., 2016; Herweg et al., 2020).

The decline in memory for associative information is a hallmark of normal human aging (Howard et al., 2006; Old and Naveh-Benjamin, 2008; Bender et al., 2010; Koen and Yonelinas, 2014; Nyberg and Pudas, 2019). However, surprisingly, whether the coordination of brain rhythms underlying associative memory formation is compromised in older adults has not yet been investigated. Hence, the goal of this study was twofold: first, to investigate whether theta-gamma coupling specifically supports the successful formation of item-context associations (as compared with item-only recognition), and second, whether age-related declines in associative memory are associated with less precise theta-gamma synchronization during memory formation.

To this end, EEGs were recorded while younger and older adults engaged in an item-context association task (Fig. 1) that involved the formation of associations between objects and scenes. In a subsequent recognition memory test, old and new objects were presented on top of old or new scenes, and participants were asked to judge whether (1) the object and (2) the

object/scene pair were old or new. Importantly, old objects were presented either superimposed on the identical scene from encoding (match condition) or on a familiar, old scene that had been paired with other objects during encoding (mismatch condition). This design ensures that correct responses in the associative condition rely on the retrieval of the association between objects and scenes, and not simply on a feeling of familiarity for the respective constituents of the association. Therefore, our design allowed us to clearly separate mechanisms of item-only recognition from those underlying associative memory.

As postulated by theory, we found that successful associative memory formation, that is, the successful subsequent retrieval of the item-context association, was preceded by a coupling of gamma power to the peak of the theta rhythm during encoding. Concurrently, item-only recognition was characterized by a shift in coupling phase, away from the peak, in both younger and older adults. Importantly, participants who showed a coupling closer to the theta peak also showed better associative memory. Finally, older adults' lower pair memory performance was accompanied by a temporal shift in coupling phase compared with that of younger adults. Together, the present results are consistent with the hypothesis that decrements in the temporal precision with which gamma power is coupled to the theta phase underlies the decline of associative memory in normal cognitive aging.

Materials and Methods

Participants. Younger ($n = 65$) and older ($n = 72$) healthy, right-handed, German-speaking adults were recruited via a database of the Max Planck Institute for Human Development to participate in the study. They received a compensation of 12 Euros per hour. A total of 24 participants were excluded because of technical problems (6), dropping out (3), noisy EEG data (1), memory performance below chance (2; see below, Behavioral analysis), and because of too few trials per condition (12; see below, EEG recording and preprocessing). The remaining sample consisted of 58 younger (33 females, $M_{age} = 25.0$, $SD_{age} = 3.1$, range 20–31 years) and 55 older adults (24 females, $M_{age} = 69.6$, $SD_{age} = 3.7$, range 64–76 years). We aimed for a minimum of 50 subjects per age group and a *post hoc* power analysis performed in G*power (Faul et al.,

2007) demonstrated that on the basis of the effect size for the age-by-condition interaction observed for performance ($\eta_P^2 = 0.04$) and on the final sample size ($n = 113$), the current study had strong statistical power (0.95). To further characterize the sample, all participants completed a demographic questionnaire and additional cognitive tests. In the Digit Symbol Substitution Test (Wechsler, 1955) measuring processing speed, younger adults attained a significantly higher score (mean = 66.24; SD = 10.79) than older adults (mean = 49.91; SD = 10.14; W = 4445, z = 6.54, $\alpha = 0.05$, $p < 0.001$). In the Spot-the-Word test (Lehrl et al., 1995) measuring verbal knowledge, the older adults (mean = 28.95; SD = 3.21) showed significantly better performance than the younger adults (mean = 22.52; SD = 3.46; W = 1989, z = −7.58, $\alpha = 0.05$, $p < 0.001$). In addition, the older adults (mean = 28.78, SD = 1.34, range = 24–30) were assessed using the Mini Mental State Examination (Folstein et al., 1975). A score of 27 or higher indicates normal cognition, whereas a score of 19–23 indicates mild cognitive impairment (O'Bryant et al., 2008). Performance in these tasks was similar to that of other cognitive neuroscience studies previously run at our research center (Sander et al., 2011; Karlsson et al., 2020) and showed a typical pattern of age differences. The Ethics Committee of the Deutsche Gesellschaft für Psychologie approved the study.

Stimuli. The experiment was programmed in MATLAB (version 2016b, MathWorks), using the Psychophysics Toolbox (Brainard, 1997). The stimulus pool consisted of 498 colored pictures (400 × 400 pixels) of everyday objects (e.g., ball, teapot; Brady et al., 2008) and 210 colored pictures (1280 × 960 pixels) of outdoor scenes (e.g., forest, beach) retrieved from the Internet (open source).

Experimental paradigm. The experiment consisted of four parts, a prelearning phase, a learning phase, a postlearning phase, and a retrieval phase, completed during 1 d with short breaks in between the sessions, including a 40 min lunch break after the learning phase. For the purpose of the present analysis, we focus on the learning and retrieval phases. However, note that the objects and scenes presented in the learning phase, and thus serving as old in the retrieval phase, had been shown in a target detection task during the prelearning phase performed in the Magnetic Resonance Imaging scanner. Furthermore, the objects were also presented in the postlearning phase in a similar target detection task.

The learning phase was performed in a dimly lit room that was electromagnetically and acoustically shielded. Participants' neural activity was recorded with EEG, and their eye movements were monitored with an eye tracker. Before the task, participants received instructions and completed two short practice rounds that were repeated if necessary. The experimental session started with written instructions on the screen, and the experimenter initiated the session with a button press.

During encoding, 250 randomly drawn objects and 50 randomly drawn scenes were presented together in an item-context association task. Each trial started with a jittered fixation cross (~1–1.5 s), followed by the presentation of a scene. Next, five objects were presented (3 s each) sequentially superimposed on the center of the scene, and each presentation was separated by a fixation cross (2 s). To ensure explicit attempts to associate objects and scenes and promote binding in both age groups (Craik and Rose, 2012; Bastin et al., 2013), participants were instructed to imagine using the presented object in the place depicted in the scene. After the presentation of the five objects, participants indicated on a three-point Likert scale how well they managed to do the task.

At test, participants were presented with the old objects intermixed with 150 randomly drawn new objects, presented on either a new ($n = 50$) or an old scene ($n = 100$). This resulted in five test conditions: old objects presented on their original scene from study (match condition, $n = 100$ trials), old objects on old but mismatching scenes from study (mismatch condition, $n = 100$ trials), old objects on new scenes (old-new condition, $n = 50$ trials), new objects on old scenes from study (new-old condition, $n = 100$ trials), and new objects on new scenes (new-new condition, $n = 50$ trials). We constrained the occurrence of old objects and scenes in the recognition test in the following ways. (1) The five objects belonging to the same learning sequence (i.e., presented on the same scene) were assigned to the three test conditions involving old objects as follows: Two objects were assigned to the match condition, two objects to the mismatch condition, and one object to the old-new condition.

Because the position of the object within the learning sequence may influence memory performance, we made sure that each condition contained an equal number of objects from each encoding position. (2) The order of trials was randomized, with the constraint that no more than three consecutive trials could stem from the same condition. (3) Each scene from encoding was presented a total of five times (within the different test conditions, see above), but never in consecutive trials during tests.

At test, each trial started with a fixation cross (0.5 s) followed by the presentation of a scene (1 s). Next, an object was presented superimposed on the center of the scene. Participants were first required to respond whether the object was old or new (maximum 3 s) and subsequently whether the specific object/scene pair was old or new (maximum 4 s). Responses were recorded using a response box, and the mapping of button to response (old/new) was counterbalanced across participants.

Behavioral analysis. Behavioral responses were analyzed as item and pair responses. First, to assess item chance-level performance, the proportion of correct item responses was calculated across all three old item conditions (match, mismatch, old-new) with the chance level set to 0.31 (derived from the multiplication of the response probability by the proportion of trials with an old item, that is, $0.5 \times 250/400 = 0.31$). Participants with performance below this chance level were excluded from the analysis. To control for response biases, item and pair memory performance were quantified as corrected recognition scores. Corrected item recognition scores (Snodgrass and Corwin, 1988) were obtained by subtracting the proportion of old item responses to new objects from the proportion of old item responses to old objects (from the match and mismatch conditions only). Similarly, corrected pair recognition scores were obtained by subtracting the proportion of old pair responses to new objects from the proportion of correct pair responses (i.e., responding old pair to an old object on a matching scene or new pair to an old object on a mismatching scene). To assess age differences in item and pair memory performance, corrected recognition scores were analyzed in a mixed-effects ANOVA, with age (younger/older) as between-subjects and condition (item/pair) as within-subjects factors. Any significant interactions were followed up by pairwise comparisons, and Bonferroni-corrected p values are reported when applicable. Finally, because correctly rejecting an old object with a mismatching scene as a new pair depends on the explicit retrieval of the association, and cannot rely on simple familiarity for the constituent parts, associative memory is most clearly emphasized in this condition. Therefore, to assess explicit associative memory and age differences therein, we compared pair false alarm rates (i.e., old pair responses) to old objects on mismatching scenes between age groups using a t test. The data were analyzed using R 3.5.2 (https://www.R-project.org/).

EEG recording and preprocessing. The EEG was recorded with the BrainVision Recorder (Brain Vision) from a 61 Ag/Ag-Cl electrodes embedded cap, which was placed according to the 10-10 system (1000 Hz sampling rate; right mastoid reference). An electrode above the forehead (AFz) served as ground. To measure eye movements with the electrooculogram, electrodes were placed below the left eye and at the left and right outer canthi. Electrode impedances were kept below 5 kΩ during the EEG measurement. In addition, participants' heart rate was recorded via electrocardiogram (ECG) to remove possible cardiovascular artifacts from the EEG signal (see below).

EEG preprocessing was performed using FieldTrip (Oostenveld et al., 2011), EEGLAB (Delorme and Makeig, 2004), and custom-written MATLAB code (MathWorks). Before preprocessing, eye movement and EEG data were merged along the time vectors to ensure equal time point zero across modalities. The EEG data were filtered (fourth filter order) with a bandpass of 1–150 Hz and rereferenced to the linked mastoid channels. The ECG data were filtered with a band-stop filter (48–52 Hz) and appended to the EEG data. Next, the data were segmented into epochs of 2 s, and each trial was visually inspected. Epochs containing strong artifacts not related to eye movements or blinks were temporarily excluded for the following independent component analysis (ICA). In addition, any channel strongly contaminated by artifacts was excluded. Blink, eye-movement, muscle, and heartbeat artifacts were detected using ICA (Bell and Sejnowski, 1995) and removed from the signal. In

Table 1. Distribution of trials per condition and age group

	Younger adults			Older adults		
	M	Min	Max	M	Min	Max
Item-only	35.6	10	57	43.6	19	74
Pair	58.7	28	109	46.8	16	89

Distribution of trials for the item-only and pair memory conditions. Mean and range are reported for each age group. M, Mean; Min, minimum; Max, maximum.

addition, saccade-related transient spike potentials were identified using the COSTRAP algorithm and removed from the signal as independent components (Hassler et al., 2011). Artifact-contaminated channels and trials (determined across all epochs) were automatically identified (1) using the FASTER algorithm (Nolan et al., 2010) and (2) by detecting outliers exceeding 4 SDs of the kurtosis of the distribution of power values in each epoch within low- (0.2–2 Hz) or high-frequency (30–100 Hz) bands, respectively. Channels labeled as artifact contaminated were interpolated using spherical splines (Perrin et al., 1989). Finally, the data were segmented into 7 s epochs, ranging from 2 s before to 5 s after stimulus onset and sorted into conditions of interest, item-only memory (i.e., objects correctly remembered without the associated scene) and pair memory (i.e., objects and the associated scene correctly remembered). A second visual inspection of each trial per participant was performed, and any remaining artifact-contaminated trials were excluded from further analysis, resulting in an average of 5.95% of trials being rejected. Participants with <10 trials per condition were excluded from the analyses. Table 1 shows the distribution of trials across conditions and age groups.

Single-trial rhythm detection and individual theta peak frequency estimation. Because phase information is only meaningful in the presence of an underlying oscillation (Aru et al., 2015), we used the extended BOSC (Better OSCillation detection) method (Whitten et al., 2011; Kosciessa et al., 2021) to identify rhythmic events in the theta frequency range (3–7 Hz) on the single-trial level. The method assumes that rhythmic events have stronger power than the 1/f background spectrum and should be present for a predefined minimum number of cycles at a given frequency. By means of robust regression, the procedure dissociates narrowband peaks from the aperiodic background spectrum (Kosciessa et al., 2020), and identifies time points per trial and channel for which the signal meets these criteria and can thus be considered to reflect an oscillation. In the present study, a three-cycle threshold was set as the temporal criterion, and the 95th percentile above the individual background spectrum was defined as the power threshold. EEG data were decomposed into 49 logarithmically spaced center frequencies between 1 and 64 Hz using a 5-cycle wavelet. The most dominant peaks between 3–7 Hz (theta) and 8–15 Hz (alpha) were removed before fitting the 1/f slopes. Next, rhythmic segments were estimated, demonstrating reliable peaks in the theta band in all subjects in both age groups (see Fig. 3a for group averages). Because theta frequency varies across individuals (Klimesch, 1999), we estimated the individual theta peak frequency to use as the phase-carrying frequency in the subsequent theta-gamma coupling analyses (for a similar approach; Friese et al., 2013; Köster et al., 2018). To this end, the power spectrum was averaged across all rhythmic segments for each channel and trial. By means of local maxima, a peak frequency was estimated per channel, and the final individual theta peak frequency range was defined as the average peak frequency across channels ± 0.5 Hz.

Next, rhythmic segments of 1 s surrounding the middle peak of the theta rhythm, as estimated by BOSC, were extracted. Peaks were detected by means of local maxima (phase > 2Π–0.1) and used to align the averaged unfiltered EEG signal and the gamma power spectrum to the time point reflecting the peak (time = 0) of the oscillation (see Figure 5b). Note that 1 s segments were chosen to cover at least three cycles of the theta center frequency (minimum 3 Hz). In addition, to avoid confounds evoked by stimulus onset, the first 0.2 s of the epochs were excluded. Finally, we grouped the rhythmic segments over the posterior channels defined as a region of interest (see Fig. 3d and below) and averaged over segments within a given trial. Similarly, nonrhythmic 1 s

segments were extracted from time periods not characterized as rhythmic by BOSC. To keep the number of rhythmic and nonrhythmic segments equal for later analysis, we randomly selected as many nonrhythmic as rhythmic segments from the total sample of nonrhythmic segments per channel and trial. Similarly, to balance the number of trials, we then randomly selected as many trials as the average across the two conditions (item-only and pair).

Next, we investigated whether the amplitude or the temporal duration of rhythmicity present during encoding differed between age groups and whether they alone already predicted subsequent item-only memory and pair memory. The temporal duration of rhythmicity present was quantified as abundance, that is, temporal duration relative to the full-time window analyzed (3 s). We conducted two separate mixed-effect ANOVAs for amplitude and abundance with age (younger/older) as between-subject and condition (item-only/pair) as within-subject factors.

Gamma power estimation. To determine the frequency range and topographical distribution of gamma band activity involved in memory encoding, we assessed gamma power increases relative to the prestimulus time period as follows: Gamma power was estimated using multitapers (7; Slepian), with a 0.4 s window length, a step size of 0.08 s, and a frequency resolution of 5 Hz. The power spectrum was log transformed at the single-trial level (Smulders et al., 2018). The peristimulus power spectrum (0–3 s) was then contrasted against the prestimulus power spectrum (−0.7 to −0.2 s), within participant. Baseline data were averaged over trials and time, and power increases were quantified by computing single-sample t statistics for any given channel–frequency–time point. To test statistical significance, the distribution of t values was tested against a null distribution on the group level using a nonparametric cluster-based permutation approach (Maris and Oostenveld, 2007). Initially, clusters were formed based on univariate, one-sided independent samples t statistics for each channel–frequency–time point. The threshold for data points to be included in a cluster was set to $p = 0.01$, and the spatial constraint was set to a minimum of two neighboring channels. Next, the significance of the summed t values was assessed in comparison to a permutation null distribution, obtained by switching the condition labels and recomputing the t test 2000 times. The final cluster p-value (i.e., the Monte Carlo significance probability) is the proportion of random partitions in which the cluster-level statistics were exceeded. The threshold was set to p values below 0.05, that is, one-sided significance threshold. The channel frequency cluster identified in this analysis (see Fig. 3d) was used to define a gamma-band region and frequency of interest for further analyses. Finally, we tested whether gamma power increases differed between age groups and between later item-only memory and pair memory. To that end, power values within the region and frequency of interest were sorted based on subsequent memory (item-only/pair, as described above), averaged across rhythmic segments, and analyzed in a mixed-design ANOVA with age (younger/older) as between-subject and condition (item-only/pair) as within-subject factors.

Cross-frequency coupling. To investigate whether gamma power increases are modulated by the theta phase, we estimated the coupling between theta phase and gamma power in the following way: To derive the phase of the theta oscillation, the preprocessed signal was filtered with a two-pass bandpass filter (filter order = 3), with a bandwidth centered at the individual peak frequency range (i.e., peak frequency ± 0.5 Hz). The analytic phase time series were estimated via Hilbert transform. To derive the instantaneous power of the modulated frequency (i.e., within in the gamma frequency range), a two-pass bandpass filter (filter order = 3) was applied from 50 to 75 Hz, comprising the frequency range showing reliable power increases during memory encoding (see Fig. 3d), in steps of 5 Hz. To avoid biased results toward slower frequencies (Aru et al., 2015), the bandwidth was set to ± 7.5 Hz. The Hilbert-derived complex signal was z scored within frequency bands to normalize amplitudes across frequencies and finally squared to estimate the instantaneous power time series. Next, the power time series were separated into rhythmic and nonrhythmic segments (see above, Single-trial rhythm detection and individual theta peak frequency estimation) and sorted into 36 phase bins (10° bin width) according to the phase time

series within a given channel and trial. To assess the presence of theta-gamma coupling, we tested for deviations from uniformity using the Rayleigh test, which evaluates whether the resultant vector length is large enough to indicate a nonuniform distribution. To this end, the phase-binned gamma power was averaged over trials, and the phase angle at which gamma power was strongest were derived for each participant and condition (item-only/pair). To assess whether gamma power is modulated by the theta phase for subsequent item-only memory and pair memory in both age groups, the Rayleigh test was applied to each condition and age group separately. In addition, the randomly selected nonrhythmic segments were used as a control condition and analyzed in a similar fashion. The Watson–Williams test, which assesses whether the mean direction (i.e., coupling phase angle) differs between two groups, was used to assess age differences in coupling phase angles. To examine whether item-only memory is characterized by a deviation in coupling phase, the absolute difference in phase angle between item-only memory and pair memory was computed for each participant. To assess the statistical significance, a phase deviation score was computed by dividing the absolute phase difference with the maximum possible value (i.e., pair – item-only / 180) and the Wilcoxon signed rank test was applied per each age group. To assess age differences in phase deviation, the Wilcoxon rank sum test was used to contrast the age groups. Finally, to examine the relationship between coupling phase and associative memory, a linear-circular correlation between individual phase angle and the proportion of correct pair responses was computed. To better illustrate the heterogeneity within our sample, we additionally performed a median split on the pair hit rates (within age groups), and theta-gamma coupling in low- and high-performing younger and older adults were examined by means of the Rayleigh test, and age groups were contrasted using the Watson–Williams test. The analysis was performed using the Circular Statistics Toolbox (Berens, 2009) and custom written MATLAB code.

Data availability . Custom MATLAB and R code of the main analyses are available from https://osf.io/vdn4r/.

Results

Older adults show reduced pair memory performance. Item and pair memory performance were quantified by corrected recognition scores. Corrected item recognition scores were obtained by subtracting the proportion of old item responses to new objects from the proportion of old item responses to old objects on matching and mismatching scenes. Corrected pair recognition scores were obtained by subtracting the proportion of old pair responses to new object pairs from the proportion of correct pair responses (i.e., responding old pair to an old object on a matching scene and new pair to an old object on a mismatching scene). To investigate whether age differences are greater for pair as compared with item memory performance, corrected recognition scores were investigated in a mixed ANOVA with age (younger/older) as between-subject and condition (item/pair) as within-subject factors. The analyses demonstrated main effects of age ($F_{(1,111)} = 4.69$, $p = 0.033$, $\eta_P^2 = 0.04$) and of condition ($F_{(1,111)} = 412.72$, $p < 0.001$, $\eta_P^2 = 0.79$), reflecting generally better item than pair memory performance in both age groups. This is a trivial finding given that item recognition is generally easier than pair memory. The finding of interest is the significant age-by-condition interaction ($F_{(1,111)} = 5.06$, $p = 0.026$, $\eta_P^2 = 0.04$). Follow-up pairwise comparisons showed that item memory performance did not differ between age groups ($p > 0.6$), whereas pair memory performance was significantly ($t_{(94.53)} = 3.53$, $p = 0.001$, d = 0.66; independent t test with Welch-modified degrees of freedom) lower in older than in younger (Fig. 2a; Table 2) adults. Finally, to isolate explicit associative memory, we investigated pair false alarms (i.e., responding old pair) to mismatching pairs, given that this condition depends on the explicit retrieval of object-scene associations. Indeed, older adults showed a higher
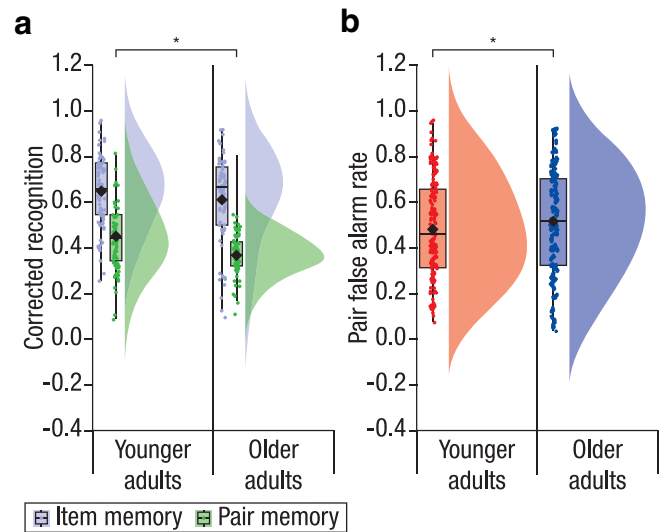
Figure 2. *a*, Corrected recognition scores (*y*-axis) for item (purple) and pair memory (green), demonstrating comparable item memory performance across age groups (*x*-axis) but reduced pair memory in older compared with younger adults. *b*, Pair false alarm rates (*y*-axis) demonstrate that older adults (blue) are more likely to incorrectly endorse old items on mismatching scenes as old pairs in comparison to younger adults (red). Box plots represent the interquartile range (first and third quantile), with dots representing individual participants. The rhombus indicates the mean, the horizontal bar indicates the median, and half-violin plots illustrate the sample density. Asterisks indicate statistical significance ($p < .05$).

Table 2. Descriptive statistics for behavioral performance

	Younger adults	Older adults
Item	0.65 (0.16)	0.61 (0.21)
Pair	0.45 (0.16)	0.36 (0.09)
False alarms	0.31 (0.13)	0.41 (0.21)

Means and SDs (in parentheses) are reported for each age group and measure.

false alarm rate than younger adults did ($t_{(88.99)} = -2.98$, $p = 0.004$, d = 0.20; independent t test with Welch-modified degrees of freedom; Fig. 2b; Table 2). Thus, we replicated the finding that item recognition remains fairly intact in old age, whereas associative memory is compromised relative to younger adults.

Clear evidence for oscillatory theta activity in younger and older adults. A prerequisite for any meaningful interpretation of phase information is the actual presence of an underlying oscillation (Aru et al., 2015). Therefore, in a first step, we established the presence of oscillatory activity in the EEG signal on the single-trial level using an extension of the BOSC method (Kosciessa et al., 2020). This method is particularly well suited for identifying rhythmic segments in the theta frequency range on the single-trial level (see above, Materials and Methods). For single-trial time windows that contained theta oscillations according to BOSC, all individuals in both age groups showed reliable peaks in the power spectrum within the theta frequency range, providing clear evidence that oscillatory theta activity was present in both age groups (see Fig. 3a, group averages of the power spectrum). Given that the frequency of theta varies across individuals (Klimesch, 1999), we estimated the individual theta peak frequency for each participant (on rhythmic data as defined by BOSC) and used it as the phase-carrying frequency in the following analyses (see above, Materials and Methods). For subsequent analyses, the data were sorted into rhythmic and nonrhythmic segments (1 s) within channels and trials based on the time windows identified as oscillatory by the BOSC algorithm. Note that we only included segments within a posterior
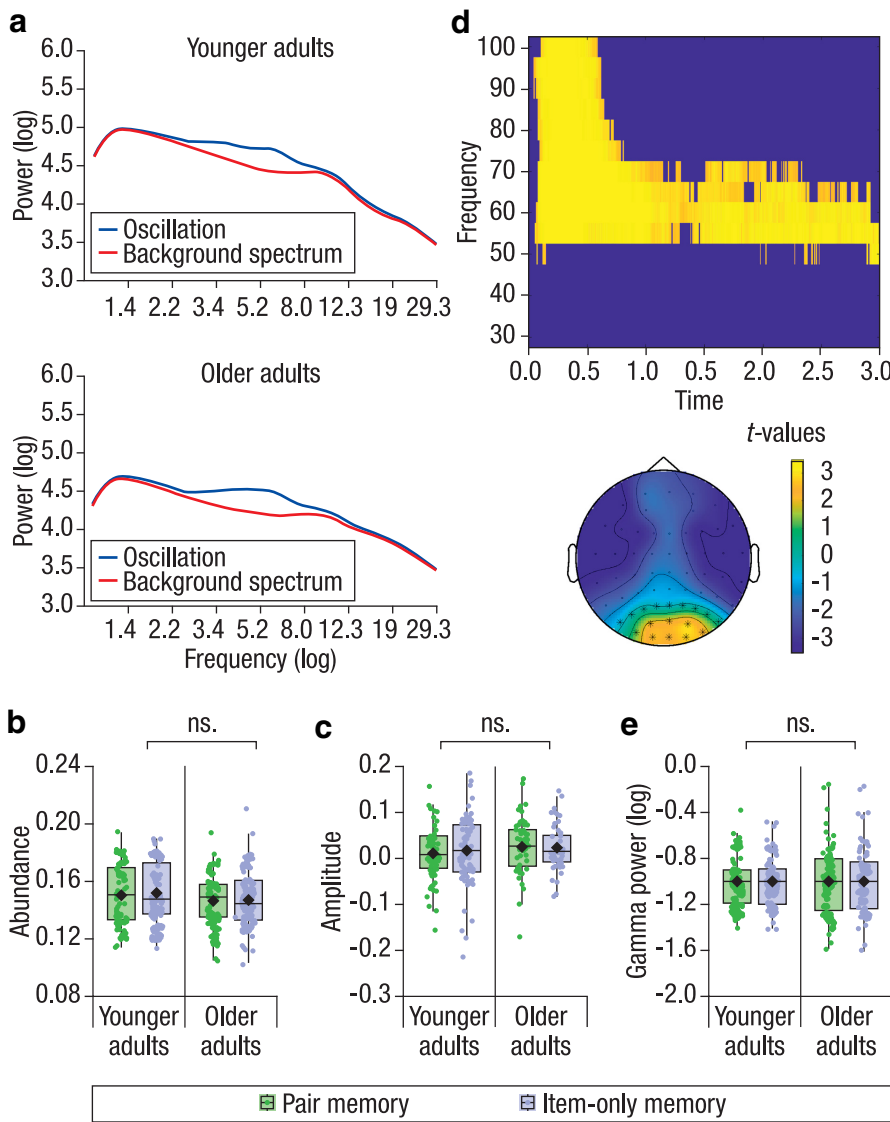
Figure 3. *a*, Younger and older adults show reliable peaks over the theta frequency range during rhythmic segments as estimated on the single-trial level. The figures illustrate power (*y-axis*) per frequency (*x*-axis), averaged over rhythmic episodes (blue) relative to the background spectrum (red). *b*, The relative amount of rhythmicity over time (i.e., abundance; *y*-axis) did not differ between age groups (*x*-axis) or between item-only memory (green) and pair memory (purple). *c*, The amplitude of the theta rhythm (*y*-axis) did not differ between age groups (*x*-axis) or between item-only memory (green) and pair memory (purple). *d*, Top, The identified time (*x*-axis) and frequency (*y*-axis) cluster during encoding showing reliable increases in gamma power relative to a prestimulus period (*t* values). Bottom, The topographical distribution of the gamma band effect averaged over time (0.4–3 s; *t* values). Asterisks highlight significant channels. *e*, Gamma power (averaged across the identified cluster over rhythmic time windows) did not differ in magnitude between age groups (*x*-axis) or between item-only memory (green) and pair memory (purple). Box plots represent the interquartile range (first and third quantile) with dots representing individual participants. The rhombus indicates the mean, and the horizontal bar indicates the median. ns indicates non-significance.

matching or mismatching scenes; hereafter, pair memory) provided data for the associative memory condition. Before investigating the interaction between activity in the theta and gamma bands, we tested whether the amplitude or the temporal duration of rhythmic theta activity present during encoding differentiated between subsequent item-only memory and pair memory, and contributed to age differences therein. Based on the BOSC method, we quantified temporal duration as abundance (Kosciessa et al., 2020), that is, the duration of a rhythm relative to the full-time window analyzed (3 s). The mixed ANOVAs with age group (younger/older) as between-subject and condition (item-only/pair) as within-subject factors showed no significant main effects or interaction effects for amplitude or abundance (*p* values > 0.28; Fig. 3*b,c*). Specifically, we did not observe age-related reductions in rhythmic theta activity per se, which means that results regarding item recognition versus associative memory were not influenced by the mere occurrence or magnitude of rhythmic activity.

Gamma power increases during memory encoding. To isolate the frequency range and topographical distribution of gamma band activity presumably representing the object information during encoding, we determined increases in neural activity during the peristimulus (0–3 s) period relative to the prestimulus (−0.7 to −0.2 s) period using a nonparametric cluster-based permutation approach. The analysis yielded a positive effect (*p* = 0.009), reflecting a sustained power increase following stimulus onset (Fig. 3*d*). The effect-carrying frequency range (50–75 Hz) and channel cluster (Pz, P1, P2, P3, P4, P5, P6, P7, P8, POz, PO3, PO4, PO7, PO8, O1, O2, Oz) was used as a region and frequency of interest for the following analyses. In an analogy to the analysis on differences in theta abundance during encoding reported above, we first examined whether differences in gamma power explained subsequent memory (item-only vs pair) or age group differences. Therefore, we quantified gamma power within the region and frequency of interest for time windows classified as rhythmic. A mixed-model ANOVA, with age (younger/older) as between-subject and condition (item-only/pair) as within-subject factors, showed no significant main effects or interactions (*p* values > 0.6; Fig. 3*e*). Thus, gamma power increases also did not show reliable differences between age groups or between subsequent item recognition and associative memory.

Theta-gamma coupling supports associative memory formation. So far, we have demonstrated reliable oscillatory activity

cluster of channels defined as the gamma region and frequency of interest (see below; Fig. 3*d*). To assess differences in oscillatory activity related to item and pair memory formation, we sorted the rhythmic data into two conditions (similar to a subsequent memory analysis; Paller and Wagner, 2002). Rhythmic segments belonging to trials for which only the object was later recognized without memory for the object–scene association (i.e., correct item responses followed by an incorrect pair response to objects on matching or mismatching scenes; henceforth item-only memory) provided data for the item recognition condition, and rhythmic segments belonging to trials for which the object–scene association was remembered (i.e., correct item responses followed by a correct pair response to old objects on

within the theta frequency range as well as reliable gamma power increases during encoding, but none of these factors showed differences between item-only and pair memory or between age groups. Next, we therefore assessed whether their interplay, namely theta-gamma CFC, would reveal differences that relate to memory performance within and between participants and age groups. To that end, gamma power was averaged over trials and within the frequency and region of interest defined by the gamma band analysis described above (see above, Gamma power increases during memory encoding), and then sorted into theta phase bins (36 bins in total; see above, Materials and Methods). An individual phase angle was derived for each participant and condition (item-only, pair) based on the distribution of gamma power across bins, reflecting the theta phase bin(s) at which gamma power is strongest. To test for a deviation from uniformity, which would indicate a modulation of gamma power by the theta phase, we applied the Rayleigh test on the samples of phase angles per age group and condition separately. Note that a similar analysis was performed on nonrhythmic segments, that is, 1 s time windows when no rhythmic theta activity was identified by BOSC, which was balanced regarding the number of trials. This analysis served as a control to demonstrate that any identified coupling was not artefactual but specifically observed when an underlying theta rhythm was present. The analysis demonstrated that both item-only memory and pair memory were associated with a reliable deviation from uniformity in younger (item-only: $z = 4.11$, $p = 0.016$, $r = 0.27$; pair: $z = 3.64$, $p = 0.026$, $r = 0.25$) and older (item-only: $z = 3.65$, $p = 0.025$, $r = 0.25$; pair: $z = 3.71$, $p = 0.024$ $r = 0.25$) adults, reflecting reliable phase–amplitude coupling between theta and gamma. Importantly, nonrhythmic segments did not show a reliable deviation from uniformity in any age group (younger: $z = 0.30$, $p = 0.74$; older: $z = 0.78$, $p = 0.46$). These results suggest that gamma power increases tend to be coupled to a specific phase of the theta rhythm during memory encoding. As illustrated in Figure 4a,b, coupling appears to occur closer to the peak of the theta cycle for pair memory compared with item-only memory in both age groups (Table 3). To investigate whether item-only memory, as characterized by the failure to retrieve the associated context, was associated with a deviation from the coupling phase that was found to be maximal, and possibly optimal, for successful pair memory formation, we computed the within-person absolute difference in coupling phase between item-only memory and pair memory (Table 3). To assess the reliability of the deviation, a phase deviation score was computed by dividing the absolute phase difference by 180 (i.e., the maximum possible difference). The Wilcoxon signed-rank test demonstrated a reliable deviation of the coupling phase in both younger ($W = 1711$, $z = 6.62$, $\alpha = 0.05$, $p < 0.001$, $r = 0.87$) and older ($W = 1540$, $z = 6.45$, $\alpha = 0.05$, $p < 0.001$, $r = 0.87$) adults, and the Wilcoxon rank sum test showed that the deviation was comparable across age groups ($p > 0.3$; Fig. 4c). Thus, in agreement with our expectations, these results demonstrate that the modulation of gamma power by the phase of the theta rhythm is specific to oscillatory time windows. Importantly, reliable theta-gamma coupling was evident in both age groups, indicating that this key mechanism of associative memory formation continues to be in effect in old age. Furthermore, in line with previous work (Kerrén et al., 2018), we show that there is an optimal theta phase for the formation of item-context associations, which is reflected in gamma power increases close to the peak of the theta oscillation in both younger and older adults. In contrast, item-only memory was characterized by more off-peak power increases in both age groups.

Coupling during associative memory formation is shifted in time in older adults. To answer the key question of whether aging is associated with a temporal shift in theta-gamma coupling, that is, whether observed gamma power increases are coupled to a different phase of the theta cycle in older than in younger adults, we contrasted the phase angles between age groups using the Watson–Williams test. The analysis demonstrated significant differences in phase angles between age groups for pair ($F_{(1,111)} = 4.81$, $p = 0.030$; $\eta^2 = 0.20$) and for item-only ($F_{(1,111)} = 20.13$, $p < 0.001$, $\eta^2 = 0.39$) memory. Thus, although both age groups tended to couple close to the peak of the theta oscillation, there was a clear temporal shift in coupling phase in older adults relative to that of younger adults. Interestingly, this age-related shift in coupling phase was evident for both subsequent item-only memory and pair memory (Fig. 4a, age comparison of the coupling phase angles; Fig. 5a, age comparison of the gamma power distributions). As illustrated in Figure 5b, younger adults showed gamma power increases more consistently around the peak of the theta rhythm, whereas older adults showed a more distributed coupling pattern. Finally, to assess whether interindividual differences in coupling phase (i.e., the theta phase at which gamma power increases were most prominent) were related to interindividual differences in pair memory performance, we computed the linear-circular correlation between the individual phase angle within pair memory trials and the proportion of correct pair responses. The analysis demonstrated a positive relationship, indicating that coupling closer to the peak of the theta oscillation was beneficial for associative memory ($r = 0.31$, $p = 0.005$; Fig. 5c). Note that the correlation remained fairly reliable within each age group (younger: $r = 0.31$, $p = 0.057$; older: $r = 0.35$, $p = 0.037$), suggesting that the relationship is not driven solely by one age group. To further understand this relationship, a median split was performed on the proportion of correct pair responses per each age group, and theta-gamma coupling during pair memory formation was assessed for high- and low-performing younger and older adults separately. The Rayleigh test demonstrated that high-performing younger adults ($z = 6.52$, $p = 0.001$; $r = 0.47$) and older adults ($z = 4.11$, $p = 0.015$; $r = 0.38$) showed reliable theta-gamma coupling, whereas neither age group of low performers did (p values > 0.29; Table 3). Further, the Watson–Williams test ($p > 0.98$) demonstrated that gamma power in high-performing older adults was as precisely coupled to the peak of the theta rhythm as in high-performing younger adults. These findings provide strong evidence for the claim that the coupling of gamma power to theta phase during encoding supports associative memory formation. In addition, the results are consistent with the hypothesis that adult age differences in associative memory reflect a decline in the temporal precision of this coupling mechanism.

Discussion

Accumulating evidence suggests that the precise coupling between gamma power increases, and the phase of rhythmic theta activation (Tort et al., 2009; Lisman and Jensen, 2013) supports the formation of associations among different elements of an event, an essential feature of episodic memory (Tulving, 2002). Normal human aging is associated with declines in episodic memory, and age differences are greatest for memory for associative information (Old and Naveh-Benjamin, 2008). Accordingly, it has been proposed that aging is associated with reductions in the ability to associate distinct elements of an episode into a coherent memory representation during encoding (Chalfonte and Johnson, 1996;
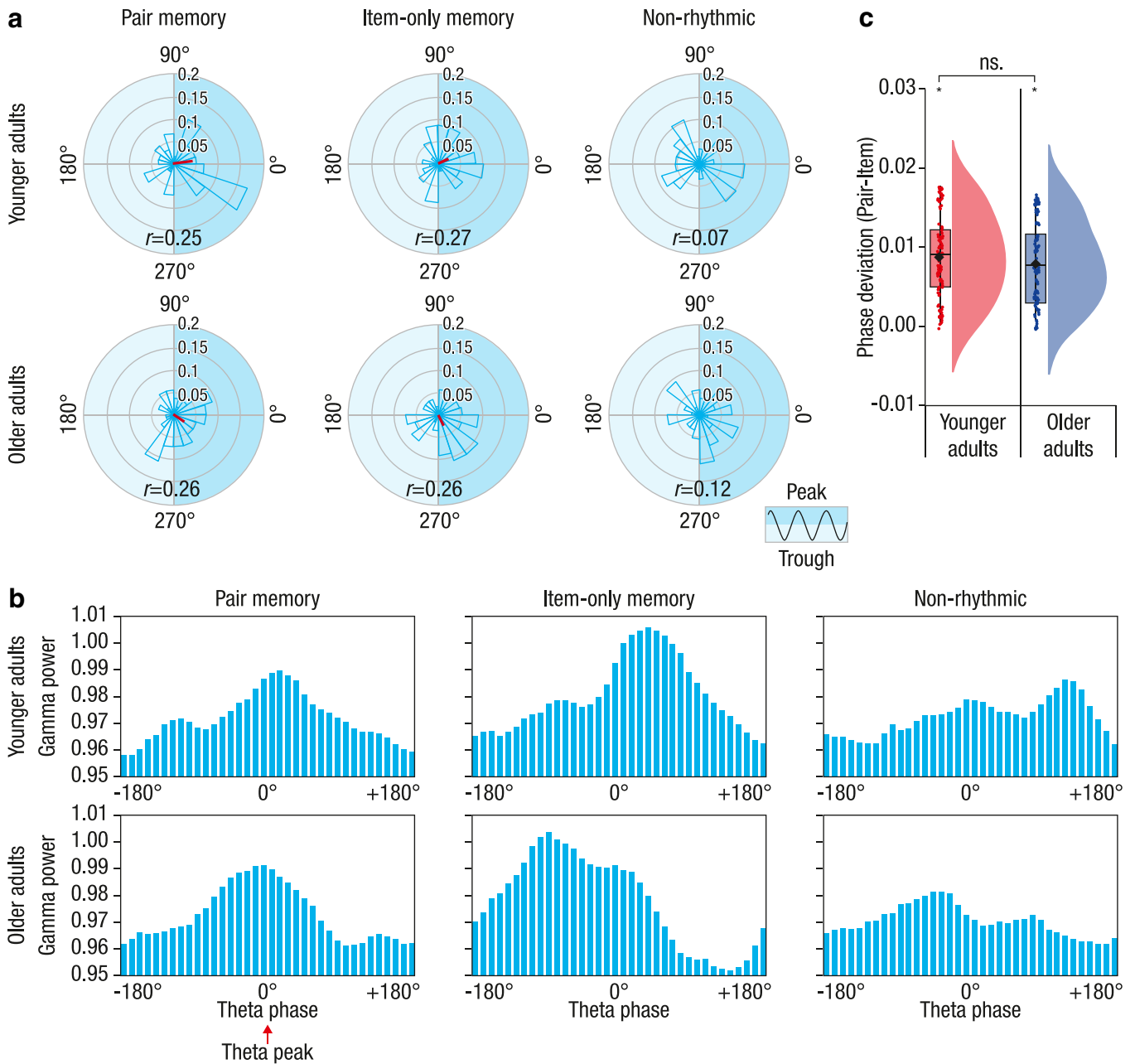
Figure 4. *a*, Angular histograms of the theta-gamma coupling phase across conditions for younger (top) and older adults (bottom). The peak of the theta cycle corresponds to phase 0° (cosine), and red lines indicate the mean direction (i.e., phase angle) and magnitude (i.e., length) of the mean resultant vector. The axis rings illustrate the proportion of individual coupling phase angles in the histogram falling in each phase bin. Note that the red line (i.e., the vector length) has been scaled accordingly, and *r* indicates the true vector length. *b*, The corresponding distributions of gamma power (*y*-axis) over theta phase bins (*x*-axis). Similarly, the peak (highlighted with red arrow) corresponds to phase 0°. *c*, The phase deviation for younger (red) and older (blue) adults Asterisks indicate statistical significance ($p < .05$) and ns indicates non-significance.. Box plots represent the interquartile range (first and third quantile) with dots representing individual participants. The rhombus indicates the mean, and the horizontal bar indicates the median. Together, the plots illustrate the presence of theta-gamma coupling during item-only memory and pair memory formation but not during nonrhythmic segments (*a*, *b*) and the age-invariant deviation in coupling phase for item-only memory compared with pair memory (*c*).

Naveh-Benjamin, 2000). However, the question of whether normal aging compromises the temporally precise theta-gamma coupling during the formation of associative memories has not been addressed thus far.

Here, we showed that theta-gamma CFC supports successful memory formation in an item-context association task in both younger and older adults. First, we documented the presence of oscillatory activity in the theta frequency range in both younger and older adults (Fig. 3*a–c*). Similarly, the increase in gamma power during encoding did not differ by age group (Fig. 3*d,e*). We then provided evidence for the key role of theta-gamma CFC

in associative memory formation by showing that gamma power is coupled to the phase of the theta rhythm during memory encoding. Theta-gamma coupling was evident regardless of whether only the item or the pair were correctly recognized at test. However, the coupling phase of trials in which later only the object was recognized (without its associated scene or item-only memory) deviated from the coupling phase of trials in which the object–scene pair (i.e., the association of the object with its scene or pair memory) was successfully retrieved (Fig. 4). In comparison to item-only memory formation, pair memory formation was characterized by gamma power increases that were closer to

Table 3. Descriptive circular statistics

	Younger adults				Older adults			
	Pair	Item-only	Phase deviation	High performing	Pair	Item-only	Phase deviation	High performing
Phase angle	10.3	26.1	90.5	346.3	325.9	294.5	80.6	346.6
Vector length	0.25	0.27	0.61	0.47	0.26	0.26	0.64	0.38
Circular variance	0.75	0.73	0.39	0.53	0.74	0.74	0.36	0.62
Circular SD	1.22	1.21	0.88	1.03	1.22	1.22	0.85	1.12
Kurtosis	0.08	0.02	−0.01	0.21	−0.06	0.12	0.04	0.07
Skewness	−0.11	0.07	−0.03	0.07	−0.09	0.10	−0.11	−0.03

Descriptive circular statistics, separated by age group, for the different conditions (pair and item-only), for the difference between them (i.e., deviation; pair/item-only), and for pair memory of the groups of high-performing individuals. Phase angle indicates the mean phase angle in degrees. The vector length indicates concentration around the mean phase angle. Circular variance and SD are circular analogs to the corresponding linear measures. Kurtosis is a measure of peakedness, and skewness indicates symmetry around the mean direction (i.e., mean phase angle).
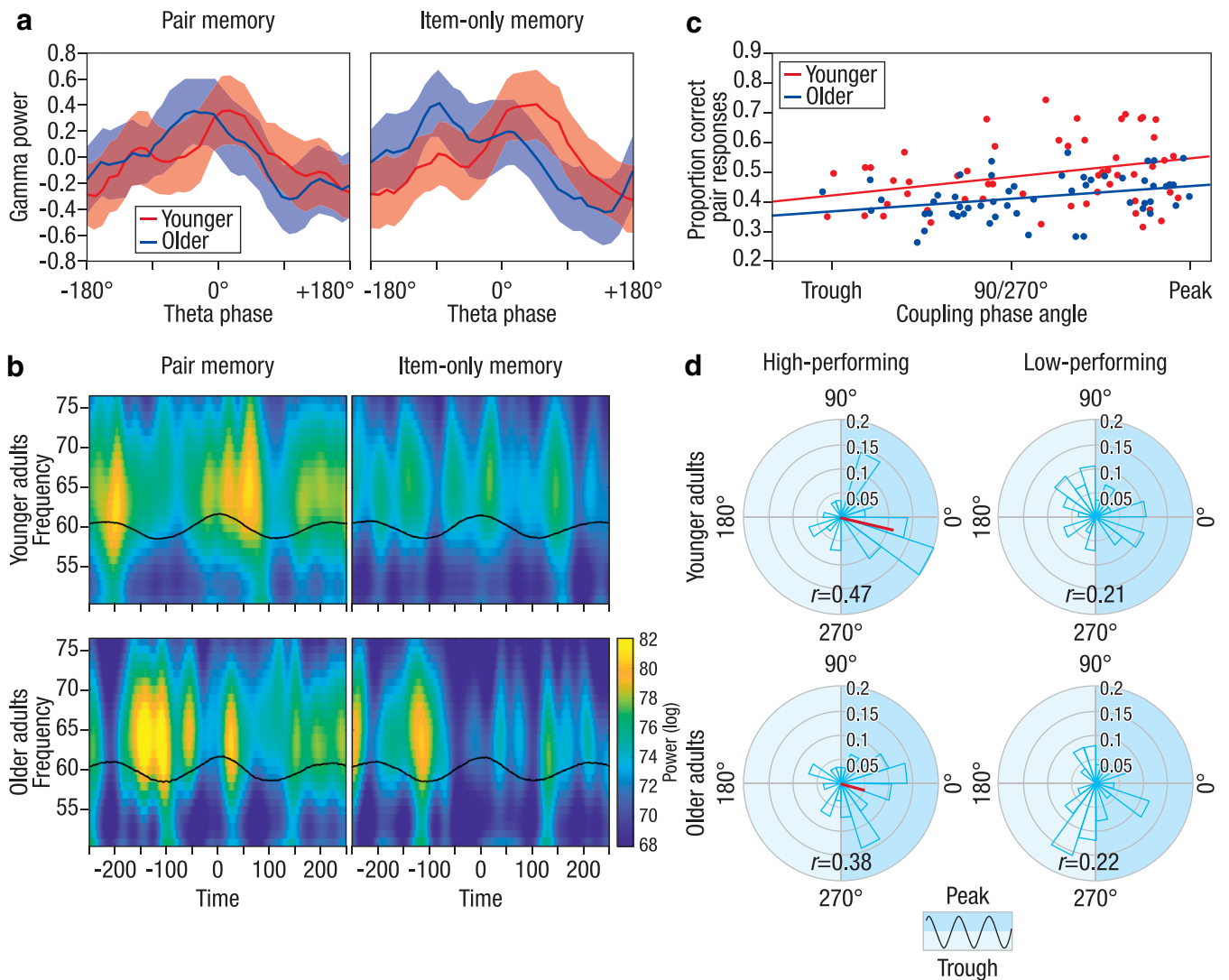
Figure 5. *a*, Illustration of age differences in the distribution of gamma power (*y*-axis) over the theta phase bins (*x*-axis) for pair memory (left) and item-only memory (right). Shaded area indicates 95% confidence interval, and phase 0° corresponds to the theta peak (cosine). The plots illustrate the temporal shift in coupling phase for older compared with younger adults. Note that the gamma power distributions from Figure 4*b* are replotted here to highlight the age differences. *b*, Illustration of the time (*x*-axis) and frequency (*y*-axis) power spectrum within the gamma band (50–75 Hz) for pair memory (left) and item-only memory (right). The black line represents a peak-locked average of the unfiltered EEG signal aligned to the middle peak (time = 0) of the theta rhythm. The plots illustrate the temporally shifted coupling in older compared with younger adults. *c*, The relationship between the proportion of correct pair responses (*y*-axis) and individual coupling phase (*x*-axis; angle in degrees). For illustrative purposes only, absolute phase angles are plotted. Colored lines and dots indicate regression lines for the two age groups and individual data points, respectively. The plot demonstrates a positive association, suggesting that coupling around the peak is beneficial for pair memory performance. *d*, Angular histograms demonstrating the greater temporal precision in coupling phase evident in high-performing compared with low-performing younger and older adults. The peak of the theta cycle corresponds to phase 0° (cosine), and red lines indicate the mean direction (i.e., phase angle) and magnitude (i.e., length) of the mean resultant vector. The axis rings illustrate the proportion of individual coupling phase angles in the histogram falling in each phase bin. Note that the red line (i.e., the vector length) has been scaled accordingly, and *r* indicates the true vector length.

the peak of theta oscillation, presumably the optimal phase for memory formation (Hasselmo, 2005; Kerrén et al., 2018). Importantly, this effect was present in both younger and older adults. Furthermore, individual differences in associative memory were correlated with individual differences in the theta coupling phase (Fig. 5c) in both age groups. Critically, we observed reliable differences in coupling phase between age groups, with older adults' lower pair memory performance being associated with a phase shift away from the theta peak (Fig. 5a,b; Fig. 4a). Together, our results support the hypothesis that normal aging compromises the temporal precision of neural communication during the formation of associative memories.

Theta-gamma coupling supports the formation of item-context associations
The nesting of gamma band activity within the theta cycle reflects the synchronization of distributed neural populations, whereby the phase of the theta cycle determines time windows of synaptic plasticity, inducing long-term potentiation and long-term depression (Pavlides et al., 1988; Hyman et al., 2003). Accordingly, leading theories on the role of a theta-gamma code in memory (Hasselmo, 2005; Lisman and Jensen, 2013; Hanslmayr et al., 2019) posit that the theta rhythm regulates the precise timing of neural activity between different cell populations and thereby promotes the strengthening of synaptic connections that serves associative memory formation. Recent work has demonstrated that theta-gamma CFC supports episodic memory contingent on contextual information (Tort et al., 2009; Heusser et al., 2016; Köster et al., 2018, 2019). However, most studies did not explicitly assess associative memory but used confidence ratings (Staudigl and Hanslmayr, 2013) or the remember/know procedure (Köster et al., 2019) to infer recollection at the time of testing. In the present design, pair memory was explicitly tested, allowing us to disentangle potential differences in CFC underlying subsequent item-only memory versus pair memory. We found that item-only versus pair memory was associated with different coupling patterns. In particular, coupling closer to the peak of the theta rhythm was beneficial for later pair memory. In contrast, when items were later recognized without memory for their associated context, we observed a reliable deviation of ~80–90° from the coupling phase optimal for successful associative memory. This finding suggests that the failure to subsequently retrieve the association between an item and its context is associated with gamma power increases occurring at a substantially different theta phase that is shifted away from the theta peak. Thus, our results extend previous findings by demonstrating that the coupling of gamma power to a specific theta phase during encoding supports the formation of item-context associations in particular. The finding that neither the temporal duration of rhythmicity in the theta band nor the strength of cortical activation in the gamma band present at encoding distinguished between subsequent item-only memory and pair memory substantiates the proposal that associative memory formation is dependent on the precise timing of the interaction between theta and gamma activity. Thus, we argue that cortical representations of item and context information, as reflected in activity in the gamma band, are bound via the theta rhythm (Clouter et al., 2017; Herweg et al., 2020), which ensure the exact timing in neural communication to lay down new associative memories.

Most prior observations of theta-gamma CFC during memory formation have been made in the hippocampus and/or the surrounding medial temporal lobe (MTL), an associative hub strongly implicated in episodic memory formation (Davachi, 2006; Eichenbaum et al., 2007; Moscovitch et al., 2016) where theta is the dominant rhythm (Buzsáki and Moser, 2013). The extent to which scalp-recorded theta reflects hippocampally versus neocortically generated theta is not fully understood. It has been suggested that cortical theta is driven by hippocampal projections (Ekstrom et al., 2005) and that synchronized gamma activity in neural assemblies across distributed cortical regions are biased by the hippocampal theta phase (Sirota et al., 2008). In addition, increased phase coherence in the theta band has been demonstrated between frontal and posterior cortical networks during the formation of item-context associations (Summerfield and Mangels, 2005; Fell and Axmacher, 2011; Burke et al., 2013) and between subregions within the MTL in support of successful memory formation (Solomon et al., 2019). Moreover, Clouter et al. (2017) showed that inducing auditory and visual oscillatory entrainment to a synchronized theta phase (i.e., with zero phase lag) was beneficial for subsequent associative memory compared with a desynchronized entrainment phase (i.e., a phase lag of 90° or more). Together, these results provide strong evidence that the theta rhythm binds together distinct pieces of information via phase synchronization, both locally and across larger spatial distances, allowing associative information to be coded by the hippocampal network. Given that the task used in the present study can be assumed to rely heavily on hippocampally mediated associative processes, it is likely that the theta-gamma coupling observed in the present study is triggered by or at least is interacting with the hippocampal network in coordinating the formation of associations between item and context information.

Lower pair memory in older adults is accompanied by a temporal shift in theta-gamma coupling
The associative deficit hypothesis posits that age-related declines in episodic memory reflect difficulties in forming associations between distinct elements of an episode (Naveh-Benjamin, 2000). Accordingly, we found that item recognition was comparable across age groups, whereas older adults showed reduced memory for associative information relative to younger adults. These age differences in pair memory performance were accompanied by age differences in coupling phase. Although coupling around the peak of the theta rhythm was beneficial for pair memory formation in both age groups, older adults showed a reliable shift in coupling phase relative to younger adults for both subsequent pair memory and item-only memory (i.e., objects later recognized with and without the associated scene. Hence, as a group, older adults consistently showed less temporally precise coupling to the optimal phase of the theta rhythm than young adults. Importantly, the observation that neither the temporal duration of rhythmicity nor gamma power increases during encoding differed between age groups further corroborates the proposal that the reduction seen in associative memory in the older age group was because of an alteration of the precise interaction between theta and gamma activity.

It may be a surprise that age differences in coupling phase were present regardless of subsequent associative memory success. However, trials here defined as item-only memory included correct item responses followed by incorrect pair responses, thus, trials in which associative information was not available or not correctly retrieved. The proportion of these trials differed between age groups, as reflected in higher false alarm rates to mismatching pairs in older compared with younger adults. Higher occurrence of these false alarms, that is, false recognition of rearranged pairs, is a common finding in aging research and

has been related to age differences in hippocampal activation (Dennis et al., 2008; Fandakova et al., 2014) and to the volume of a subregion of the hippocampus (DG/CA3; Shing et al., 2011) that supports episodic memory formation (O'Reilly and McClelland, 1994). Accordingly, the observed age differences in CFC for item-only memory likely reflect the increased rates of false alarms in older adults resulting from an attenuated coding of the association by the hippocampal system. In addition, it is noteworthy that the deviation in coupling phase for item-only memory showed different directions for younger and older adults. Although we argue that the premature coupling phase in the older adults likely reflects the associative deficit, we speculate that the delayed coupling in the younger adults may reflect other failures preventing good encoding, such as attentional lapses (deBettencourt et al., 2018; Fiebelkorn and Kastner, 2019).

Our results add to previous findings indicating that disruptions in the dynamics of neural communication underlie senescent cognitive changes (Voytek and Knight, 2015). Previously, decreased synchrony in the theta band between frontal and posterior regions (Tóth et al., 2014), and altered synchronization between theta and gamma activity (Pinal et al., 2015; Reinhart and Nguyen, 2019), has been associated with reduced working memory performance in older adults. The present results extend these observations of compromised neural communication as a marker of age-related cognitive decline to the domain of episodic memory formation. At the same time, it is important to note that those older adults who showed a more youthlike theta-gamma coupling pattern also showed better associative memory, as revealed by a stable relationship between individual coupling phase and the proportion of correct pair responses (compare Nyberg et al., 2012; Fandakova et al., 2015; Muehlroth et al., 2019). In fact, among high-performing older adults, coupling occurred as precisely to the peak of the theta rhythm as among high-performing younger adults. This is in line with the proposal that cognitive performance in old age is determined by the level of preservation of neural structures and functionally specialized processes (Nyberg et al., 2012; Nyberg and Pudas, 2019; Nyberg and Lindenberger, 2020). In particular, maintenance of hippocampal structure may preserve hippocampally mediated functions such as the precise timing of neural synchronization in high-performing older adults. Thus, although the temporal dispersion in theta-gamma CFC contributes to age-related declines in associative episodic memory, older adults who are able to preserve a youthlike coupling pattern also maintain their episodic memory function to a greater extent. However, when the neural system fails to consistently couple to the optimal phase of the theta rhythm, the induction of synaptic plasticity is attenuated, and the coding of associative information by the MTL is compromised, resulting in reductions of associative memory performance with advancing adult age.

Finally, it is noteworthy that neurotransmitters, for example, dopamine and norepinephrine, have been shown to modulate neural plasticity (Lisman and Grace, 2005; O'Dell et al., 2015), and recent work suggests that dopamine may modulate the coupling between higher and lower frequencies (Andino-Pavlovsky et al., 2017). In addition, individual differences in episodic memory have been related to differences in neurotransmitter function (Bäckman et al., 2010; Nyberg et al., 2016). Thus, individual differences in the stability of the underlying neurochemical system may be a contributing factor to the observed differences in the temporal precision of theta-gamma coupling. Future work may focus on the link between age-related changes in neuromodulating transmitters and theta-gamma coupling, and the relation to hippocampus-dependent associative processes.

Conclusion

Prominent neurocognitive theories of memory have long suggested that rhythmic modulations of synchronized neural excitability serve neural communication and that reductions in the precision of cross-frequency coupling come at a cost for cognitive performance. Here, we show that during the formation of item-context associations, gamma power increases are coupled to an underlying theta rhythm in both younger and older adults. Coupling closer to the peak of the theta rhythm is associated with better pair memory, pointing to a phase angle that is optimal for facilitating associative binding. Older adults showed lower pair memory performance and a large deviation from younger adults' mean phase direction. At the same time, high-performing older adults showed more youthlike patterns of theta-gamma coupling. The present pattern of findings is consistent with the hypothesis that normal aging compromises the temporal precision of neural communication, leading to age-related impairments in the formation of episodic memories.

References

Andino-Pavlovsky V, Souza AC, Scheffer-Teixeira R, Tort ABL, Etchenique R, Ribeiro S (2017) Dopamine modulates delta-gamma phase-amplitude coupling in the prefrontal cortex of behaving rats. Front Neural Circuits 11:29.

Aru J, Aru J, Priesemann V, Wibral M, Lana L, Pipa G, Singer W, Vicente R (2015) Untangling cross-frequency coupling in neuroscience. Curr Opin Neurobiol 31:51–61.

Bäckman L, Lindenberger U, Li SC, Nyberg L (2010) Linking cognitive aging to alterations in dopamine neurotransmitter functioning: recent data and future avenues. Neurosci Biobehav Rev 34:670–677.

Bastin C, Diana RA, Simon J, Collette F, Yonelinas AP, Salmon E (2013) Associative memory in aging: the effect of unitization on source memory. Psychol Aging 28:275–283.

Battaglia FP, Benchenane K, Sirota A, Pennartz CMA, Wiener SI (2011) The hippocampus: hub of brain network communication for memory. Trends Cogn Sci 15:310–318.

Bell AJ, Sejnowski TJ (1995) An information-maximization approach to blind separation and blind deconvolution. Neural Comput 7:1129–1159.

Bender AR, Naveh-Benjamin M, Raz N (2010) Associative deficit in recognition memory in a lifespan sample of healthy adults. Psychol Aging 25:940–948.

Berens P (2009) CircStat: a MATLAB toolbox for circular statistics. J Stat Soft 31:1–21.

Brady TF, Konkle T, Alvarez GA, Oliva A (2008) Visual long-term memory has a massive storage capacity for object details. Proc Natl Acad Sci U S A 105:14325–14329.

Brainard DH (1997) The Psychophysics Toolbox. Spatial Vis 10:433–436.

Burke JF, Zaghloul KA, Jacobs J, Williams RB, Sperling MR, Sharan AD, Kahana MJ (2013) Synchronous and asynchronous theta and gamma activity during episodic memory formation. J Neurosci 33:292–304.

Buzsáki G, Wang X-J (2012) Mechanisms of gamma oscillations. Annu Rev Neurosci 35:203–225.

Buzsáki G, Moser EI (2013) Memory, navigation and theta rhythm in the hippocampal-entorhinal system. Nat Neurosci 16:130–138.

Buzsáki G, Logothetis N, Singer W (2013) Scaling brain size, keeping timing: evolutionary preservation of brain rhythms. Neuron 80:751–764.

Canolty RT, Knight RT (2010) The functional role of cross-frequency coupling. Trends Cogn Sci 14:506–515.

Chalfonte BL, Johnson MK (1996) Feature memory and binding in young and older adults. Mem Cogn 24:403–416.

Clouter A, Shapiro KL, Hanslmayr S (2017) Theta phase synchronization is the glue that binds human associative memory. Curr Biol 27:3143–3148.e6.

Craik FIM, Rose NS (2012) Memory encoding and aging: a neurocognitive perspective. Neurosci Biobehav Rev 36:1729–1739.

Davachi L (2006) Item, context and relational episodic encoding in humans. Curr Opin Neurobiol 16:693–700.

deBettencourt MT, Norman KA, Turk-Browne NB (2018) Forgetting from lapses of sustained attention. Psychon Bull Rev 25:605–611.

Delorme A, Makeig S (2004) EEGLAB: an open source toolbox for analysis of single-trial EEG dynamics including independent component analysis. J Neurosci Methods 134:9–21.

Dennis NA, Hayes SM, Prince SE, Madden DJ, Huettel SA, Cabeza R (2008) Effects of aging on the neural correlates of successful item and source memory encoding. J Exp Psychol Learn Mem Cogn 34:791–808.

Eichenbaum H, Yonelinas AP, Ranganath C (2007) The medial temporal lobe and recognition memory. Annu Rev Neurosci 30:123–152.

Ekstrom AD, Caplan JB, Ho E, Shattuck K, Fried I, Kahana MJ (2005) Human hippocampal theta activity during virtual navigation. Hippocampus 15:881–889.

Fandakova Y, Lindenberger U, Shing YL (2014) Deficits in process-specific prefrontal and hippocampal activations contribute to adult age differences in episodic memory interference. Cereb Cortex 24:1832–1844.

Fandakova Y, Lindenberger U, Shing YL (2015) Maintenance of youth-like processing protects against false memory in later adulthood. Neurobiol Aging 36:933–941.

Faul F, Erdfelder E, Lang A-G, Buchner A (2007) G*Power 3: a flexible statistical power analysis program for the social, behavioral, and biomedical sciences. Behav Res Methods 39:175–191.

Fell J, Axmacher N (2011) The role of phase synchronization in memory processes. Nat Rev Neurosci 12:105–118.

Fiebelkorn IC, Kastner S (2019) A rhythmic theory of attention. Trends Cogn Sci 23:87–101.

Folstein MF, Folstein SE, McHugh PR (1975) "Mini-mental state": a practical method for grading the cognitive state of patients for the clinician. J Psychiatr Res 12:189–198.

Fries P (2005) A mechanism for cognitive dynamics: neuronal communication through neuronal coherence. Trends Cogn Sci 9:474–480.

Friese U, Köster M, Hassler U, Martens U, Trujillo-Barreto N, Gruber T (2013) Successful memory encoding is associated with increased cross-frequency coupling between frontal theta and posterior gamma oscillations in human scalp-recorded EEG. Neuroimage 66:642–647.

Guderian S, Düzel E (2005) Induced theta oscillations mediate large-scale synchrony with mediotemporal areas during recollection in humans. Hippocampus 15:901–912.

Hanslmayr S, Staresina BP, Bowman H (2016) Oscillations and episodic memory: addressing the synchronization/desynchronization conundrum. Trends Neurosci 39:16–25.

Hanslmayr S, Axmacher N, Inman CS (2019) Modulating human memory via entrainment of brain oscillations. Trends Neurosci 42:485–499.

Hasselmo ME (2005) What is the function of hippocampal theta rhythm?—Linking bahavioral data to phasic properties of field potential and unit recording data. Hippocampus 15:936–949.

Hassler U, Trujillo Barreto N, Gruber T (2011) Induced gamma band responses in human EEG after the control of miniature saccadic artifacts. Neuroimage 57:1411–1421.

Hebb DO (1949) The organization of behavior. New York: Wiley.

Herweg NA, Solomon EA, Kahana MJ (2020) Theta oscillations in human memory. Trends Cogn Sci 24:208–227.

Heusser AC, Poeppel D, Ezzyat Y, Davachi L (2016) Episodic sequence memory is supported by a theta-gamma phase code. Nat Neurosci 19:1374–1380.

Howard MW, Kahana MJ, Wingfield A (2006) Aging and contextual binding: modeling recency and lag recency effects with the temporal context model. Psychon Bull Rev 13:439–445.

Hyman JM, Wyble BP, Goyal V, Rossi CA, Hasselmo ME (2003) Stimulation in hippocampal region CA1 in behaving rats yields long-term potentiation when delivered to the peak of theta and long-term depression when delivered to the trough. J Neurosci 23:11725–11731.

Jutras MJ, Buffalo EA (2010) Synchronous neural activity and memory formation. Curr Opin Neurobiol 20:150–155.

Karlsson AE, Wehrspaun CC, Sander MC (2020) Item recognition and lure discrimination in younger and older adults are supported by alpha/beta desynchronization. Neuropsychologia 148:107658.

Kerrén C, Linde-Domingo J, Hanslmayr S, Wimber M (2018) An optimal oscillatory phase for pattern reactivation during memory retrieval. Curr Biol 28:3383–3392.e6.

Klimesch W (1999) EEG alpha and theta oscillations reflect cognitive and memory performance: a review and analysis. Brain Res Rev 29:169–195.

Koen JD, Yonelinas AP (2014) The effects of healthy aging, amnestic mild cognitive impairment, and Alzheimer's disease on recollection and familiarity: a meta-analytic review. Neuropsychol Rev 24:332–354.

Kosciessa JQ, Grandy TH, Garrett DD, Werkle-Bergner M (2020) Single-trial characterization of neural rhythms: potential and challenges. Neuroimage 206:116331.

Kosciessa JQ, Lindenberger U, Garrett DD (2021) Thalamocortical excitability modulation guides human perception under uncertainty. Nat Commun 12:2430.

Köster M, Finger H, Graetz S, Kater M, Gruber T (2018) Theta-gamma coupling binds visual perceptual features in an associative memory task. Sci Rep 8:1–9.

Köster M, Martens U, Gruber T (2019) Memory entrainment by visually evoked theta-gamma coupling. Neuroimage 188:181–187.

Kota S, Rugg MD, Lega BC (2020) Hippocampal theta oscillations support successful associative memory formation. J Neurosci 40:9507–9518.

Lehrl S, Triebig G, Fischer BANS (1995) Multiple choice vocabulary test MWT as a valid and short test to estimate premorbid intelligence. Acta Neurologica Scandinavica, 91:335–345.

Lisman JE, Grace AA (2005) The hippocampal-VTA loop: controlling the entry of information into long-term memory. Neuron 46:703–713.

Lisman JE, Jensen O (2013) The theta-gamma neural code. Neuron 77:1002–1016.

Maris E, Oostenveld R (2007) Nonparametric statistical testing of EEG- and MEG-data. J Neurosci Methods 164:177–190.

Markram H, Lübke J, Frotscher M, Sakmann B (1997) Regulation of synaptic efficacy by coincidence of postsynaptic APs and EPSPs. Science 275:213–215.

Miller J, Watrous AJ, Tsitsiklis M, Lee SA, Sheth SA, Schevon CA, Smith EH, Sperling MR, Sharan A, Asadi-Pooya AA, Worrell GA, Meisenhelter S, Inman CS, Davis KA, Lega B, Wanda PA, Das SR, Stein JM, Gorniak R, Jacobs J (2018) Lateralized hippocampal oscillations underlie distinct aspects of human spatial memory and navigation. Nat Commun 9:2423.

Moscovitch M, Cabeza R, Winocur G, Nadel L (2016) Episodic memory and beyond: the hippocampus and neocortex in transformation. Annu Rev Psychol 67:105–134.

Muehlroth BE, Sander MC, Fandakova Y, Grandy TH, Rasch B, Shing YL, Werkle-Bergner M (2019) Precise slow oscillation–spindle coupling promotes memory consolidation in younger and older adults. Sci Rep 9:1–15.

Naveh-Benjamin M (2000) Adult age differences in memory performance: tests of an associative deficit hypothesis. J Exp Psychol Learn Mem Cogn 26:1170–1187.

Nolan H, Whelan R, Reilly RB (2010) FASTER: fully automated statistical thresholding for EEG artifact rejection. J Neurosci Methods 192:152–162.

Nyberg L, Pudas S (2019) Successful memory aging. Annu Rev Psychol 70:219–243.

Nyberg L, Lindenberger U (2020) Brain maintenance and cognition in old age. In: The cognitive neurosciences (Poeppel D, Mangun G, Gazzaniga M, eds), pp 81–89. Cambridge, MA: MIT.

Nyberg L, Lövdén M, Riklund K, Lindenberger U, Bäckman L (2012) Memory aging and brain maintenance. Trends Cogn Sci 16:292–305.

Nyberg L, Karalija N, Salami A, Andersson M, Wåhlin A, Kaboovand N, Köhncke Y, Axelsson J, Rieckmann A, Papenberg G, Garrett DD, Riklund K, Lövdén M, Lindenberger U, Bäckman L (2016) Dopamine D2 receptor availability is linked to hippocampal-caudate functional connectivity and episodic memory. Proc Natl Acad Sci U S A 113:7918–7923.

O'Bryant SE, Humphreys JD, Smith GE, Ivnik RJ, Graff-Radford NR, Petersen RC, Lucas JA (2008) Detecting dementia with the mini-mental state examination in highly educated individuals. Arch Neurol 65:963–967.

O'Dell TJ, Connor SA, Guglietta R, Nguyen PV (2015) β-Adrenergic receptor signaling and modulation of long-term potentiation in the mammalian hippocampus. Learn Mem 22:461–471.

O'Reilly RC, McClelland JL (1994) Hippocampal conjunctive encoding, storage, and recall: avoiding a trade-off. Hippocampus 4:661–682.

Old SR, Naveh-Benjamin M (2008) Differential effects of age on item and associative measures of memory: a meta-analysis. Psychol Aging 23:104–118.

Oostenveld R, Fries P, Maris E, Schoffelen JM (2011) FieldTrip: open source software for advanced analysis of MEG, EEG, and invasive electrophysiological data. Comput Intell Neurosci 2011:1–9.

Paller KA, Wagner AD (2002) Observing the transformation of experience into memory. Trends Cogn Sci 6:93–102.

Pavlides C, Greenstein YJ, Grudman M, Winson J (1988) Long-term potentiation in the dentate gyrus is induced preferentially on the positive phase of θ-rhythm. Brain Res 439:383–387.

Perrin F, Pernier J, Bertrand O (1989). Spherical splines for scalp potential and current density mapping. Electroencephalogr Clin Neurophysiol 72:184–187.

Pinal D, Zurrón M, Díaz F, Sauseng P (2015) Stuck in default mode: inefficient cross-frequency synchronization may lead to age-related short-term memory decline. Neurobiol Aging 36:1611–1618.

Reinhart RMG, Nguyen JA (2019) Working memory revived in older adults by synchronizing rhythmic brain circuits. Nat Neurosci 22:820–827.

Sander MC, Werkle-Bergner M, Lindenberger U (2011) Binding and strategic selection in working memory: a lifespan dissociation. Psychol Aging 26:612–624.

Shing YL, Rodrigue KM, Kennedy KM, Fandakova Y, Bodammer N, Werkle-Bergner M, Lindenberger U, Raz N (2011) Hippocampal subfield volumes: age, vascular risk, and correlation with associative memory. Front Ag Neurosci 3:1–8.

Sirota A, Montgomery S, Fujisawa S, Isomura Y, Zugaro M, Buzsáki G (2008) Entrainment of neocortical neurons and gamma oscillations by the hippocampal theta rhythm. Neuron 60:683–697.

Smulders FTY, ten Oever S, Donkers FCL, Quaedflieg CWEM, van de Ven V (2018) Single-trial log transformation is optimal in frequency analysis of resting EEG alpha. Eur J Neurosci 48:2585–2598.

Snodgrass JG, Corwin J (1988) Pragmatics of measuring recognition memory: applications to dementia and amnesia. J Exp Psychol Gen 117:34–50.

Solomon EA, Stein JM, Das S, Gorniak R, Sperling MR, Worrell G, Inman CS, Tan RJ, Jobst BC, Rizzuto DS, Kahana MJ (2019) Dynamic theta networks in the human medial temporal lobe support episodic memory. Curr Biol 29:1100–1111.e4.

Staudigl T, Hanslmayr S (2013) Theta oscillations at encoding mediate the context-dependent nature of human episodic memory. Curr Biol 23:1101–1106.

Summerfield C, Mangels JA (2005) Coherent theta-band EEG activity predicts item-context binding during encoding. Neuroimage 24:692–703.

Tort ABL, Komorowski RW, Manns JR, Kopell NJ, Eichenbaum H (2009) Theta-gamma coupling increases during the learning of item-context associations. Proc Natl Acad Sci U S A 106:20942–20947.

Tóth B, Kardos Z, File B, Boha R, Stam CJ, Molnár M (2014) Frontal midline theta connectivity is related to efficiency of WM maintenance and is affected by aging. Neurobiol Learn Mem 114:58–69.

Tulving E (2002) Episodic memory: from mind to brain. Annu Rev Psychol 53:1–25.

Voytek B, Knight RT (2015) Dynamic network communication as a unifying neural basis for cognition, development, aging, and disease. Biol Psychiatry 77:1089–1097.

Wechsler D (1955) Manual for the Wechsler adult intelligence scale. New York: Psychological Corporation.

Whitten TA, Hughes AM, Dickson CT, Caplan JB (2011) A better oscillation detection method robustly extracts EEG rhythms across brain state changes: the human alpha rhythm as a test case. Neuroimage 54:860–874.

Yaffe RB, Kerr MSD, Damera S, Sarma SV, Inati SK, Zaghloul KA (2014) Reinstatement of distributed cortical oscillations occurs with precise spatiotemporal dynamics during successful memory retrieval. Proc Natl Acad Sci U S A 111:18727–18732.